Journal of Medicinal Chemistry

Article

pubs.acs.org/jmc

Life Beyond Kinases: Structure-Based Discovery of Sorafenib as Nanomolar Antagonist of 5-HT Receptors

Xingyu Lin,[†,‡] Xi-Ping Huang,[§] Gang Chen,[∥] Ryan Whaley,[§] Shiming Peng,[†] Yanli Wang,[†] Guoliang Zhang,[∥] Simon X. Wang,[⊥] Shaohui Wang,[∥] Bryan L. Roth,[§] and Niu Huang*[,†]

[†]National Institute of Biological Sciences, Beijing, No. 7 Science Park Road, Zhongguancun Life Science Park, Beijing 102206, China

[‡]College of Life Sciences, Beijing Normal University, No. 19 Xinjiekouwai Street, Beijing 100875, China

[§]Department of Pharmacology and Division of Medicinal Chemistry and Natural Products, The University of North Carolina, Chapel Hill, North Carolina 27759, United States

[∥]BeiGene (Beijing) Co., Ltd., No. 30 Science Park Road, Zhongguancun Life Science Park, Beijing 102206, China

[⊥]Department of Pharmaceutical Sciences, Howard University, Washington, D.C. 20059, United States

Supporting Information

ABSTRACT: Of great interest in recent years has been computationally predicting the novel polypharmacology of drug molecules. Here, we applied an "induced-fit" protocol to improve the homology models of 5-HT_{2A} receptor, and we assessed the quality of these models in retrospective virtual screening. Subsequently, we computationally screened the FDA approved drug molecules against the best induced-fit 5-HT_{2A} models and chose six top scoring hits for experimental assays. Surprisingly, one well-known kinase inhibitor, sorafenib, has shown unexpected promiscuous 5-HTRs binding affinities, K_i = 1959, 56, and 417 nM against 5-HT_{2A}, 5-HT_{2B}, and 5-HT_{2C}, respectively. Our preliminary SAR exploration supports the predicted binding mode and further suggests sorafenib to be a novel lead compound for 5HTR ligand discovery. Although it has been well-known that sorafenib produces anticancer effects through targeting multiple kinases, carefully designed experimental studies are desirable to fully understand whether its "off-target" 5-HTR binding activities contribute to its therapeutic efficacy or otherwise undesirable side effects.

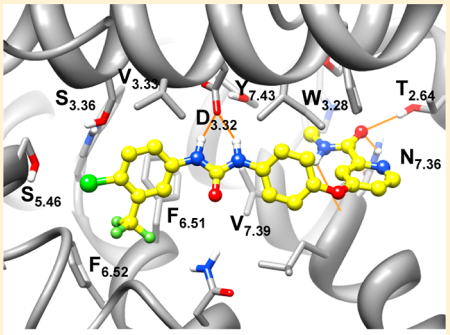

Modeled 5-HT_{2A}-Sorafenib complex structure

1. INTRODUCTION

Currently, target-based drug discovery is typically defined as "one compound−one target−one disease" with the idea that deliberately designed single-target drugs may hold the promise to specifically bind their target with reduced side effects due to off-target actions. However, single-target drugs often turn out to be less effective in treating complicated diseases such as cancers, metabolic disorders, and central nervous system (CNS) diseases.[1,2] Furthermore, many compounds designated as target-specific drugs are in fact not that selective and subsequently have been discovered to bind to other targets with similar binding affinities.[3−5] To better and more efficiently identify effective compounds that work through either known or undiscovered mechanisms, of great interest in recent years has been the development of computational methods to predict the promiscuous binding propensities of drug molecules.[6−9]

G protein-coupled receptors (GPCRs) and kinases are two of the most important drug target families. Many of their ligands are well-known to have promiscuous binding propensities within their own protein families. For example, as one of the most efficacious atypical antipsychotic drugs discovered half a century ago, clozapine binds to dozens of GPCRs with nM affinity[10] and its clinical efficacy is certainly associated with its broad target binding profile.[1,10] Similarly, the first "magic bullet" approved by the FDA for the treatment of chronic myeloid leukemia, gleevec, was initially developed to specifically inhibit the abnormal tyrosine kinase BCR-ABL. However, it was shown subsequently to target several other kinases simultaneously, including c-KIT and PDGFR.[4,5] Historically, GPCR ligands and kinase inhibitors have been developed in quite distinct chemical spaces,[11] and the selectivity panel screening campaign has generally been limited to within the same protein family members. Thus, as far as we are aware, the ligand cross-reactivity between GPCR orthosteric ligands and kinase inhibitors has not been previously reported.

The 5-hydroxytryptamine receptors (5-HTRs) are composed of 14 GPCRs in five families (5-HT1, 2, 4, 5, 6, and 7) and one ligand-gated ion channel (5-HT_3). Among 5-HTRs, the 5-HT_{2A} receptor is one of the most studied serotonergic receptors, and its inhibition is generally associated with antipsychotic and antidepressive effects.[12] In addition, the 5-HT_{2A} receptor also plays a role in thermoregulation, sleep, cardiovascular function, and muscle contraction.[13−17] A typical 5-HT_{2A} antagonist

Received: January 15, 2012
Published: June 13, 2012

 © 2012 American Chemical Society

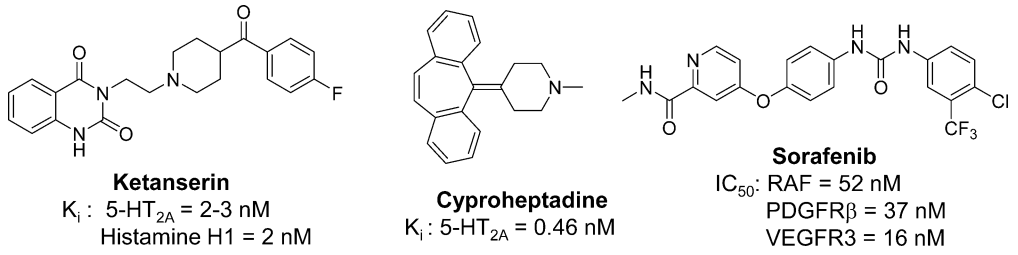

Figure 1. Chemical structures of ketanserin, cyproheptadine, and sorafenib with activity data of their known primary targets.

consists of two aryl rings and a positively charged nitrogen atom (Figure 1) and generally can be divided into class I antagonists characterized by a basic nitrogen atom in the center of the molecule and in linear disposition with the aryl rings (e.g., ketanserin) or class II antagonists with a triangular arrangement of aryl rings and a basic nitrogen (e.g., cyproheptadine).[18] Currently, very few 5-HTR ligands are subtype-selective, and the development of novel 5-HT antagonists with better specificity is highly desirable. However, this has been compromised by the lack of experimental structures of 5-HTRs.

High-resolution crystal structures of GPCRs have been published in recent years,[19] in addition to the pioneering structures of rhodopsin,[20] which greatly facilitates the GPCR structure−function study and drug discovery.[19,21] Much research is now engaged in using the available structural information for homology modeling the 3D structures of GPCRs and subsequently for docking screening and lead compound optimization purposes.[22−29]

Here we combine homology modeling, molecular docking, and molecular dynamics simulation methods to predict the potential 5-HT$_{2A}$ off-target activity of FDA approved drugs, which has not been investigated previously. We employed an "induced-fit" protocol to simulate the receptor conformational changes upon binding with two representative 5-HT$_{2A}$ antagonists. We asked whether such induced-fit models can be used to enrich known ligands from decoy molecules in retrospective virtual screening. We then asked whether we could discover potential novel polypharmacology in a prospective docking screening of FDA drug molecules.

2. METHODS

5-HT$_{2A}$ Comparative Modeling. The crystal structure (PDB code: 3D4S)[30] of the inverse agonist bound β2-adrenoceptor (β2-AR) was chosen as template to model the inactive 5-HT$_{2A}$ structure using the comparative modeling program MODELLER (version 9v7).[31] The β2 receptor has higher homology with the 5-HT$_{2A}$ receptor than with rhodopsin and has been suggested as a better template for homology modeling.[25] The sequence alignment was retrieved from GPCRDB[32] and CDD database[33] with the extracellular loop 2 (ECL2) included and the conserved disulfide bond patched, while four residues at the N terminal and five residues at the C terminal of the third intracellular loop were treated as gaps in sequence alignment to avoid the generation of linkage between transmembrane helix (TM) 5 and TM6 during structure prediction (Figure S1 in Supporting Information). The best quality model was identified with most residues located in the favored regions assessed by Ramachandran plot using Maestro (Schrödinger LLC, New York NY). The ECL2 loop and the third intracellular loop were deleted after the generation of the homology model to avoid interference from the less accurately modeled loops to the subsequent molecular docking and MD simulation. The same strategy has been applied in other GPCR modeling projects.[34,35]

Binding-Site Refinement. Instead of docking to the comparative model directly, we deliberately modified the receptor structure to incorporate knowledge of "induced-fit" effects associated with varying 5-HT$_{2A}$ antagonists' scaffolds.[36,37] Although 5-HT$_{2A}$ ligands are structurally quite diverse, the majority of 5-HT$_{2A}$ antagonists belong to class I and class II antagonists. Specifically, we chose ketanserin as the representative ligand of the class I antagonist and cyproheptadine as the class II antagonist, and we applied an induced-fit protocol (Figure 2) to sample the receptor conformational changes upon binding ketanserin and cyproheptadine, respectively.

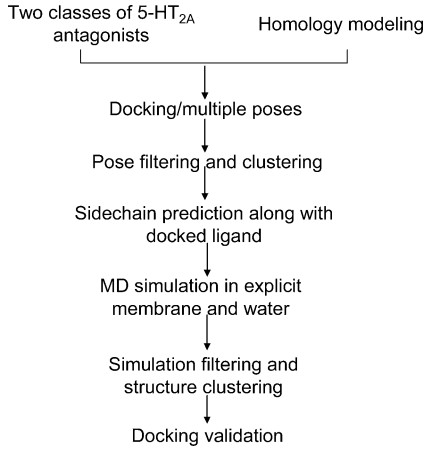

Figure 2. Our step-by-step induced-fit protocol to improve the 5-HT$_{2A}$ homology model for bound ligands.

The ligand was docked into the modeled 5-HT$_{2A}$ binding-site using the DOCK 3.5.54 program, a flexible-ligand method that uses a force-field-based scoring function.[38,39] The ligand binding-site residues were defined as in a consensus aminergic binding-site residue set, which includes 12 residues on TM3 (3.32, 3.33, 3.37, and 3.40), TM5 (5.42, 5.43, 5.46, and 5.47), TM6 (6.51 and 6.52), and TM7 (7.42 and 7.43).[40] We adopted the default parameter settings from an automated docking platform as described previously[41−43] in which all tasks including sphere generation, scoring grid, and docking calculations are driven automatically and the same docking protocol was used in the subsequent docking screenings. At this step, we saved all the docking poses for further structural analysis.

Docking poses of ketanserin and cyproheptadine were filtered by the 5 Å distance criteria between the positively charged nitrogen atom of the ligand and negatively charged carboxylate oxygen atom of D$_{3.32}$. The resulting poses were clustered into dissimilar structural groups using the DBSCAN algorithm[44] where the minimum spanning number was set to 5 or 10 points and a rmsd cutoff value of 1.5 or 2 Å for cyproheptadine and ketanserin, respectively, was applied individually. One single representative docking pose was identified from each structural cluster by choosing the most highly ranked pose that exhibits a reasonable binding mode in the binding site. Finally, 12 diverse docking poses were selected for ketanserin and four for cyproheptadine.

We submitted the selected dissimilar docking poses to a MM-GB/SA refinement and rescoring procedure,[45−50] where the side chain of binding-site residues were sampled along with the docked ligand using Protein Local Optimization Program (PLOP).[51−53] Note that in our

dx.doi.org/10.1021/jm300338m | J. Med. Chem. 2012, 55, 5749−5759

previously published works, the protein was kept rigid during minimization of the ligand−protein complex; here, we attempted to sample the side chain conformational changes with the presence of the docked ligand.[28,36,50] The docked complex structure was minimized first, followed by the side chain prediction of the binding-site residues within 5 Å of the ligand, and then the ligand was minimized with the fixed protein structure. The binding-site "induced-fit" complex structure was utilized as the starting point for further global structure refinement via molecular dynamics (MD) simulation including explicit lipid membrane and water environment.

Global "Induced-Fit" via MD Simulation. All molecular dynamic simulations were performed using the Desmond software package[54] and the OPLS-AA 2005 force field.[55] Using the default Schrödinger protein membrane building protocol, a 10 Å buffered orthorhombic boundary system was built with a POPC lipid membrane and SPC water and then neutralized by ions. The default Schrödinger protein membrane equilibration protocol was applied before production run. Briefly, each system was minimized using 2000 steps of steepest descent algorithm, followed by L-BGFS algorithm. Temperature was gradually increased from 0 to 300 K, while 50 kcal·mol^{-1} ·Å $^{-2}$ harmonic position restraints were applied to all heavy atoms of the protein and ligand during system equilibration. The restraints were gradually removed and the production run was performed in MTK-NPT (1 bar, 300 K) ensemble for 20 ns. The M-SHAKE algorithm[56] was applied to constrain all bonds involving hydrogen atoms with a time step of 2 fs. The short-range electrostatic and Lennard-Jones interactions were cut off at 9 Å. Long-range electrostatic interactions were computed by the particle mesh Ewald (PME) method[57] using a 64 × 64 × 64 grid with σ equal to 2.18 Å . Analysis of the MD simulations focused on structural and energetic properties averaged over the 10 ns production simulation. Structural analysis was performed using the UCSF Chimera[58] and VMD[59] programs, including standard root-mean-square differences (RMSDs), atom contacts, and hydrogen bonding analysis.

Model Assessment by Retrospective Docking Screening. We next investigated the ability of our induced-fit models to enrich known ligands of the 5-HT$_{2A}$ receptor. Forty-three structurally diverse 5-HT$_{2A}$ antagonists were collected from references, and molecules were prepared for docking using the latest version of the ZINC protocol.[60] Twenty decoy compounds were selected for each ligand from an in-house screening compound library (170000 compounds) based on the DUD protocol,[41] leading to a total of 774 nonredundant decoys that were physically similar but topologically dissimilar to the 43 annotated ligands (both ligands and decoy molecules are available at http://www.huanglab.org.cn/5-HT2A). Our automatic docking screening protocol was applied in default setting for each modeled receptor structure. Enrichment performance represents the prioritization of ligands among the top ranks of a docking-ordered library. We assessed the quality of the 20 induced-fit models by the early enrichment of annotated ligands from a background of decoy molecules..

Prospective Virtual Screening of FDA Drugs. We compiled a FDA drug library by merging the drug molecules from DrugBank (version 2.0)[61] and ZINC FDA drug subset (version 2005)[60] with excluding the molecules with molecular weight larger than 600 or smaller than 100 Da. A total of 1430 unique molecules were screened against two receptor models by applying our automatic docking and MM-GB/SA rescoring protocol, individually.[47−49] Note that only a single docking pose with the best total docking energy score was rescored for each molecule entry to reduce the computation cost; ultimately, we will test the docking screening capacity to rescore multiple docking poses by including the receptor binding-site flexibility. We saved the top 200 hits from MM-GB/SA scoring method for further structural analysis and visual check.

To simulate the stringent scenario with which to discover potential novel polypharmacology, we excluded the top scoring molecules with any potential GPCR-related activities such as ligands of monoamine GPCRs, monoamine transporters, and opioid receptors. All the activity data was retrieved from publicly available resources, including ChEMBL database[62] and DrugBank.[61] In addition, we also submitted identified hits to the Similarity Ensemble Approach (SEA, http://sea.bkslab.org/) server to avoid the selection of structurally similar compounds of known GPCR ligands.[7,63] SEA makes use of the chemical fingerprints of annotated ligands, calculates the similarity score between each set of ligands, and ranks the significance of the similarity scores using a rigorous statistical model.

Experimental Assays. The detailed description of experimental assays is included in the Supporting Information. Briefly, the experimental binding assays were performed by the National Institute of Mental Health's Psychoactive Drug Screening Program (PDSP) following the standard protocol. The radiolabeled reference compounds ([^{3}H]8-OH-DPAT for 5-HT$_{1A}$; [^{3}H]GR127543 for 5-HT$_{1B}$ and 5-HT$_{1D}$; [^{3}H]5-HT for 5-HT$_{1E}$; [^{3}H]Ketanserin for 5-HT$_{2A}$; [^{3}H]LSD for 5-HT$_{2B}$ and 5-HT$_{2C}$, 5-HT$_{5a}$, 5-HT$_6$, and 5-HT$_7$; [^{3}H]LY278584 for 5-HT$_3$) are used in K_i determination. The PDSP online data entry and analysis system calculates the variance of the quadruplicate determinations (for the total, nonspecific, and test compound binding values) and variances greater than 20% are flagged for further inspection and assays are repeated if necessary.

3. RESULTS AND DISCUSSION

5-HT$_{2A}$ Induced-Fit Models upon Binding with Ketanserin and Cyproheptadine. Previous computational studies have demonstrated that incorporating ligand information, binding-site residue mutation data, and molecular dynamics simulations improves the quality of GPCR structure prediction and ligand docking.[26] It is likely that the receptor undergoes conformational changes to accommodate different ligands, and rigid docking against one particular receptor conformation may be of limited utility in identifying a diverse set of ligands. The majority of 5-HT$_{2A}$ antagonists belong to class I and class II antagonists, therefore, we choose ketanserin and cyproheptadine to represent the typical 5-HT$_{2A}$ antagonists. We systematically improved the homology model in the context of these two ligands, and we assessed the extent of such ligand-induced conformational differences and revealed further details of ligand binding. We expect that the binding modes of class I and class II antagonists are similar to ketanserin and cyproheptadine, respectively.

Although the position of the orthosteric ligand binding site is conserved in the aminergic GPCRs, the detailed atomic interactions with binding site residues vary quite considerably.[40] It has been suggested that 5-HT$_{2A}$ ligands may bind into two different sites.[64,65] Site 1 is bordered by TM3, 4, 5, and 6, and site 2 is flanked by TM1, 2, 3, and 7. The shared region between site 1 and site 2 includes residues D$_{3.32}$ and S$_{3.36}$ on TM3, and W$_{6.48}$ and F$_{6.51}$ on TM6.[65] In aminergic GPCRs, the conserved D$_{3.32}$ forms a salt bridge with the tertiary amine of the ligand, which is critical for ligand binding.[66] Therefore, we generated a wide range of docking poses at the initial docking stage, followed by eliminating the misdocked poses using the conserved salt-bridge interaction as a criterion. Further structural clustering significantly reduced the redundant docking poses and eventually led to 12 dissimilar poses for ketanserin and four poses for cyproheptadine. Consistent with previous suggestions, our docking results indicate that ketanserin adopts extended conformations that allow binding in both sites, while cyproheptadine mainly binds in site 1 (Figure 3). The binding site refinement procedure did not introduce large structural perturbation; however, the side chain prediction within the binding pocket along with the docked ligand is an effective approach to maximize the interactions between binding-site residues and docked ligand and thus provides a physically reasonable complex structure for subsequent molecular dynamics simulation.

dx.doi.org/10.1021/jm300338m | J. Med. Chem. 2012, 55, 5749−5759

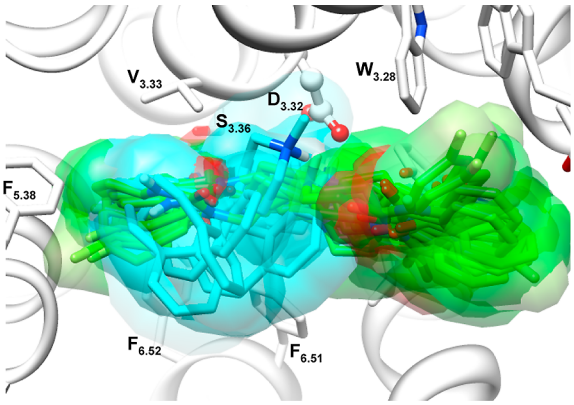

Figure 3. Overlapped diverse representative docking poses of ketanserin and cyproheptadine in the binding site of the initial homology model of 5-HT$_{2A}$. Cyproheptadine (carbon atoms colored cyan) mainly binds in site 1, mainly bordered by TM3, 5, and 6, while ketanserin (colored green) adopts extended conformations that allow binding both sites.

On the basis of docking and refinement results alone, it is difficult to determine the correct binding orientation for ketanserin. The anchoring interaction is the salt bridge between the piperidine basic nitrogen of the ligand with carboxylate group of $D_{3.32}$; however, it appears reasonable that either the *p*-fluorobenzoyl ring or quinazolinedione moiety binds in site 1 (Figure 3). Therefore, this limitation stimulated the development of the improved protein–ligand complex models in a more realistic treatment using the unbiased molecular dynamics simulation approach. We expect that multiple independent simulations can significantly increase the sampling of the complex structure, and the near-native system will be the stable system with favorable interactions between ligand and receptor and satisfies the experimental evidence like site-directed mutagenesis data.

In addition to the critical residue $D_{3.32}$, the binding site residues important for ketanserin binding have been extensively studied by mutagenesis experiments. The $F_{6.51}$L mutant decreases ketanserin binding by at least 800-fold, and the $W_{6.48}$A mutant decreases only 7-fold, while $S_{3.36}$A/C and $F_{6.52}$L mutations were found to have almost no effect on ketanserin binding affinity.[67−70] Structure–activity relationship (SAR) studies on ketanserin analogues have been shown that the hydrogen bonding capability of the quinazolinedione ring has only minor contributes to the binding affinity.[71] Furthermore, it is suggested that an ionic lock ($R_{3.50}$ And $E_{6.30}$) forms in aminergic GPCRs to stabilize the receptor in an inactive conformation.[20] Also, conserved residue $Y_{7.43}$ forms a stable hydrogen bond with $D_{3.32}$ in all known GPCR crystal structures. Therefore, we defined six structural descriptors to assess the simulation quality of each ketanserin system during the last 10 ns simulation, including the formation of salt-bridge interaction between ternary amine of ligand and conserved residue $D_{3.32}$, the absence of hydrogen bond between ligand and hydroxyl of residue $S_{3.36}$, larger ratio of vdw contacts between ligand and $Phe_{6.51}$ in comparison to $Trp_{6.48}$ and $Phe_{6.52}$, the formation of conserved ionic lock between $R_{3.50}$ and $E_{6.30}$ residues, and the presence of a stable hydrogen bond between $Y_{7.43}$ and $D_{3.32}$. We also compared the average MM-GBSA binding energies of different systems. A single simulation system (designated as Ket-6) was eventually chosen on the basis of satisfying all these available experimental evidence and energetic calculation results while the rest of the systems do not agree with at least one of the descriptors (Figure 4); the detailed analysis are also summarized in the Supporting Information (Table S1).

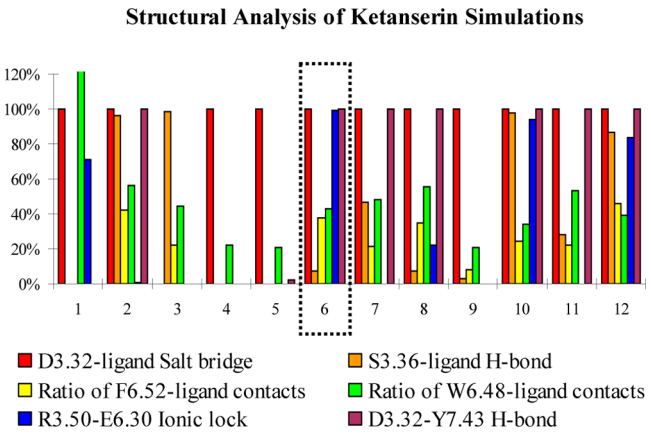

Figure 4. The structural descriptors used to assess the simulation quality of ketanserin complex systems. The *Y* axis is the measured probability of forming a specific interaction during 10 ns production simulation. The formation of D3.32–ligand salt-bridge interaction is defined as the distance between carboxylate oxygen atom of D3.32 and the piperidine nitrogen atom of ligand less than 3.5 Å, the hydrogen bond between ligand and hydroxyl of residue $S_{3.36}$ is defined by the distance of donor and acceptor less than 3.5 Å and angle greater than 120° (same for D3.32–Y7.43 hydrogen bond), the ratio of F6.52–ligand contacts is defined by the number of atom pairs within vdW contact distance between ligand and F6.52 divided by the number of atom pairs between ligand and F6.51 (same for W6.48–ligand contacts), and the R3.50–E6.30 ionic lock is defined by distance less than 4 Å between CZ atom of R3.50 and CD atom of E6.30.

In the Ket-6 system (Figure 5A), the *p*-fluorobenzoyl moiety binds in site 1, forming favorable hydrophobic interaction with $F_{6.51}$ but relatively fewer contacts with $W_{6.48}$ and $F_{6.52}$. The quinazolinedione group binds in site 2, establishing aromatic stacking interaction with $W_{3.28}$ without forming any stable hydrogen bonds in the binding site; the positively charged piperidine nitrogen forms a strong salt-bridge interaction with $D_{3.32}$ throughout the entire simulation, and $S_{3.36}$ only interacts transiently with the carbonyl group of the *p*-fluorobenzoyl ring. Nevertheless, the last 10 ns simulation trajectory in the Ket-6 simulation was clustered, a representative structure from each of the 10 largest conformational ensembles was selected, and resulted in a total of 10 representative model structures for docking evaluation.

Because of its relatively rigid structure, determination of the binding mode of cyproheptadine is less uncertain. We still assess the simulation quality using the conserved salt-bridge interaction between the positively charged nitrogen of the ligand and $D_{3.32}$, as well as the ionic lock between $R_{3.50}$ and $E_{6.30}$ and the hydrogen bond between $D_{3.32}$ and $Y_{7.43}$. Only one simulation system (designated as Cyp-4) satisfies the structural requirements (data not shown) and additionally exhibits more favorable hydrophobic interaction between the bound ligand and binding site residues (Figure 5B). Cyproheptadine mainly binds in site 1 deeply, forming strong hydrophobic interaction with $V_{3.33}$, $F_{5.38}$, $W_{6.48}$, $F_{6.51}$, and $F_{6.52}$ while maintaining its critical ionic interaction with $D_{3.32}$. Similarly, we clustered the last 10 ns simulation trajectory in the Cyp-4 simulation and

dx.doi.org/10.1021/jm300338m | J. Med. Chem. 2012, 55, 5749−5759

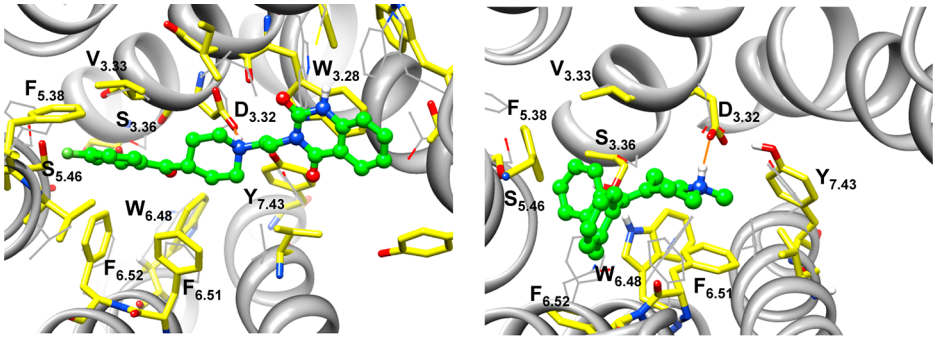

Figure 5. Conformational changes upon binding ligands ketanserin (A) and cyproheptadine (B). Induced-fit model (stick, carbon atoms colored yellow) is superimposed on the initial homology model (thin line, carbon atoms colored gray), highlighting the binding-site conformational changes in molecular dynamics simulation. The transmembrane helixes in the initial homology model are shown in ribbon representation and are omitted in the induced-fit models for clarity purpose. Carbon atoms of ligands are colored in green. The salt-bridge interaction between the tertiary amine of the ligand and the conserved D3.32 is illustrated with orange lines. Molecular images were generated with UCSF Chimera.

Table 1. Enrichments of the 43 5-HT$_{2A}$ Ligands among a Background of 774 "DUD" Style Decoy Molecules by Docking against Ketanserin and Cyproheptadine Induced-Fit Models[a]

	Ket-models									
	1	2	3	4	5	6	7	8	9	10
EF_1	2.3	0.0	0.0	0.0	0.0	4.6	4.6	0.0	2.3	0.0
EF_5	0.5	0.5	0.5	0.0	0.0	1.4	2.3	0.9	0.9	0.9
	Cyp-models									
	1	2	3	4	5	6	7	8	9	10
EF_1	2.3	0.0	4.6	4.6	1.0	2.3	0.0	2.3	4.6	2.3
EF_5	1.4	0.9	1.9	3.3	1.0	2.3	2.3	3.3	2.3	1.9

[a] EF_1 (enrichment factor at 1% of the ranked database) and EF_5 (enrichment factor at 5% of the database) present the early enrichment performance.

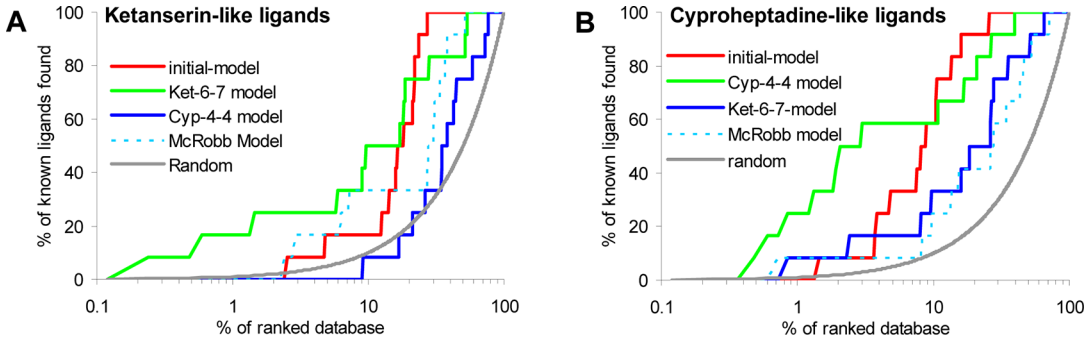

Figure 6. The enrichment profile of percentage of ligands found (*y*-axis) plotted as a function of the percentage of the ranked docked database (*x*-axis in logarithmic scale).

selected a representative structure from each of the 10 largest clusters for docking evaluation.

Assessing Induced-Fit Models by Retrospective Docking Screening. We next investigate the docking enrichment performance of a total of 20 5-HT$_{2A}$ induced-fit models. The early enrichment results are presented using EF_1 (enrichment factor at 1% of the ranked database) and EF_5 (enrichment factor at 5% of the ranked database) (Table 1). The best early enrichment performances are achieved for the seventh representative structure from the Ket-6 simulation (designated as Ket-6−7) with EF_1 of 4.6 and EF_5 of 2.3, and for the fourth representative structure from the Cyp-4 simulation (designated as Cyp-4−4) with EF_1 of 4.6 and EF_5 of 3.3, respectively. During the docking screening, it was frequently observed that one class of ligand was favored over others, indicating that different receptor conformations may be required for extensive virtual screening studies, which is exactly the case in our study. Thus, we further extracted two subsets of antagonists as ketanserin-like set and cyproheptadine-like set on the basis of structural similarity (Table S2 in Supporting Information), and we expected that the ketanserin-like ligands should be better enriched by the corresponding ketanserin induced-fit models, and similarly in cyproheptadine cases. Indeed, the early enrichment was significantly improved for the same group of ligands against the corresponding induced-fit models (Figure 6). Thus, 16.7% and 25% of the ketanserin-like ligands can be found in the top 1% and 5% of the ranked database by docking against Ket-6−7 model, respectively, corresponding to enrichment factors of 16.7 and 5. A significantly better enrichment occurs when docking against

dx.doi.org/10.1021/jm300338m | J. Med. Chem. 2012, 55, 5749−5759

Cyp-4−4 model, as 25% and 58.3% of the cyproheptadine-like ligands are found in the top 1% and 5% of the docking ranked database, corresponding to enrichment factors of 25 and 11.7.

We were also interested in comparing the docking enrichment performance of two induced-fit models to the initial comparative model and to a previously published 5-HT_{2A} induced-fit model structure.[28] Clearly, enrichments are much better in docking screening against our induced-fit models than the original homology model and one published model using exactly the same group of ligands and decoy molecules (Figure 6). In addition, we visually checked the docking poses of these ligands based on the assumption that the binding modes of class I and class II antagonists shall be similar to ketanserin and cyproheptadine, respectively. Our results (Supporting Information Table S2) demonstrate that the ligand docked to its corresponding induced-fit model typically superimposes well with its reference molecule (91% success rate for cyproheptadine-like ligands and 73% for ketanserin-like ligands), while the binding orientation by docking to the initial homology model is frequently incorrect (only 45% and 36% of success rate, correspondingly). It was encouraging that our induced-fit models are reliable for typical 5-HT_{2A} antagonist binding geometry prediction and enrichment studies, and we are confident that the same induced-fit protocol can be applied to model 5-HT_{2A} atypical antagonist bound conformations. Nevertheless, the Ket-6−7 and Cyp-4−4 models, each corresponding to one class of 5-HT_{2A} ligands, were chosen for subsequent docking screening of FDA drug molecules. The structural coordinates of both induced-fit models are freely available online (http://www.huanglab.org.cn/5-HT2A).

Prospective Virtual Screening of FDA Drugs and Experimental Validation. We then docked FDA drug molecules against both modeled 5-HT_{2A} structures and checked the top 200 compounds based on MM-GB/SA energy scores. For the present study, we mainly focused on analyzing and testing the docking results from Cyp-4−4 model due to its better enrichment performance and pose fidelity prediction in our retrospective virtual screening. First, we filtered out compounds without forming favorable hydrogen bonding interaction with residue $Asp_{3.32}$, resulting in 99 remaining molecules. Unsurprisingly, 73 molecules among these 99 compounds belong to annotated ligands of monoaminergic GPCRs, opioid GPCRs, or their corresponding membrane transporters (Supporting Information Table S3) such as phentolamine (ranking 10, α adrenergic receptor blocker), mesoridazine (ranking 14, 5-HT_{2A} and D2 receptor antagonist), and epinastine (ranking 27, histamine receptor antagonist). The aminergic GPCRs share the same or similar cognate ligands such as serotonin, dopamine, and epinephrine, and drugs targeting these receptors display broad cross-reactivity. Therefore, we eliminated all these 73 monoamine drugs related to GPCR receptors, and we were interested in discovering unexpected cross-reactivity between completely unrelated protein targets regarding the sequence, functional, and structural similarity. Finally, six drugs (Supporting Information Table S4) were selected based on commercial availability and submitted to radiolabel competitive binding assay. Among them, one kinase drug, sorafenib (Figure 1), ranks 85 in the original score list, 37 after structural filtering and 9 after activity annotation check.

Sorafenib was purchased from LC Laboratories (Woburn, MA), and the remaining five drug compounds were purchased from Sigma-Aldrich (Supporting Information Table S4). The vendors had verified the compound purity >95% by liquid chromatography−mass spectrometry (LC-MS) or nuclear magnetic resonance (NMR) experiments. The ^{1}H NMR spectrum and LC-MS data for sorafenib are included in Supporting Information Figure S2 to further validate its structure and purity. The primary screening results indicate that two compounds show a radiolabeled ligand replacement ratio larger than 20% at 10 μM concentration and sorafenib exhibits 88% inhibition. Subsequent secondary dose−response experiments indicate that sorafenib binds to 5-HT_{2A} with K_i value of 1959 nM (Figure 7). The cellular functional assay

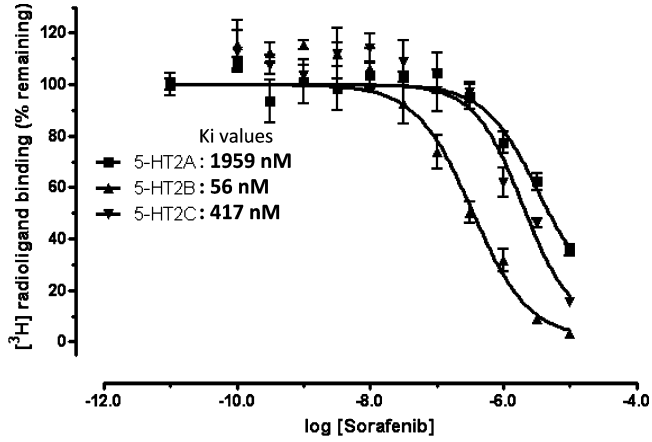

Figure 7. Radioligand competition binding assays of sorafenib. K_i value is calculated as: $K_i = IC_{50}/(1 + L/K_d)$ (Cheng−Prusoff equation), in which [L] = the radioligand concentration used in the binding assay and K_d is the affinity of radioligand at corresponding receptor. [^{3}H]-Ketanserin was used for 5-HT_{2A} binding; [^{3}H]-LSD for 5-HT_{2B} and 5-HT_{2C} binding. For 5-HT_{2A}, [L] = 3.54 nM and K_d = 2.2 nM; for 5-HT_{2B}, [L] = 2 nM and K_d = 0.5 nM; for 5-HT_{2C}, [L] = 2 nM and K_d = 0.6 nM.

validated sorafenib as a 5-HT_{2A} antagonist with 93.3 ± 1.4% of inhibition activity at 50 μM concentration. Remarkably, further 5-HTR profiling results suggest that sorafenib is a promiscuous 5-HTR ligand (Table 2), strongly binds to 5-HT_{2B} and 5-HT_{2C}

Table 2. The 5-HTRs Binding Profile of Sorafenib[a]

	receptor						
	5-HT_{1A}	5-HT_{2A}	5-HT_{2B}	5-HT_{2C}	5-HT_{5a}	5-HT_6	5-HT_7
K_i (nM)	1181	1959	56.0	417.0	3296	6213	7071

[a]Note that data represent K_i (nM) values obtained from nonlinear regression of radioligand competition binding isotherms. K_i values were calculated from best fit IC_{50} values using the Cheng−Prusoff equation.

with K_i values of 56 and 417 nM (Figure 7), and weakly binds to other five 5-HTRs including 5-HT_{1A}, 5-HT_{2A}, 5-HT_{5a}, 5-HT_6, and 5-HT_7, while it does not bind to 5-HT_{1B}, 5-HT_{1E}, 5-HF_{1F}, and 5-HT_3. Although at the current stage, it is not clearly whether sorafenib binds to other monoaminergic GPCRs, but it is highly likely to do so considering the ligand promiscuity among the monoaminergic GPCR family.

5-HT_{2A}−Sorafenib Binding Mode. Here we examine in more depth the docked complex structure of sorafenib, focusing on its chemical composition and binding mode (Figure 8A). Compared to the predicted ketanserin and cyproheptadine

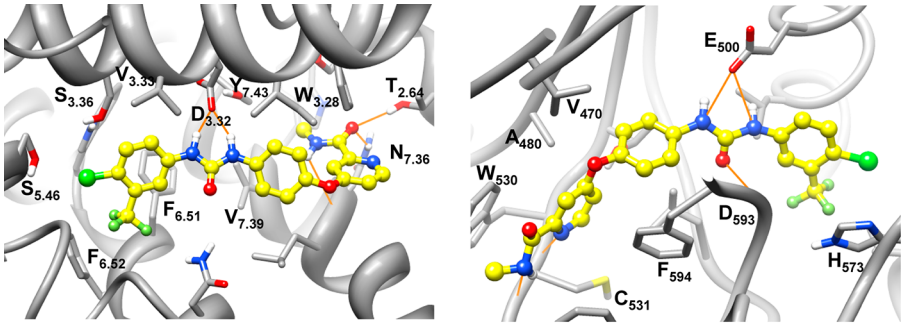

Figure 8. The binding mode of sorafenib in the modeled 5-HT_{2A}–sorafenib complex structure and the BRAF–sorafenib crystal complex structure. Carbon atoms of sorafenib are colored in yellow. The hydrogen bond interactions between the urea group of the sorafenib and the conserved D3.32 in 5-HT_{2A} (A) or the catalytic residue E500 in BRAF (B) are illustrated with orange lines. Molecular images were generated with UCSF Chimera.

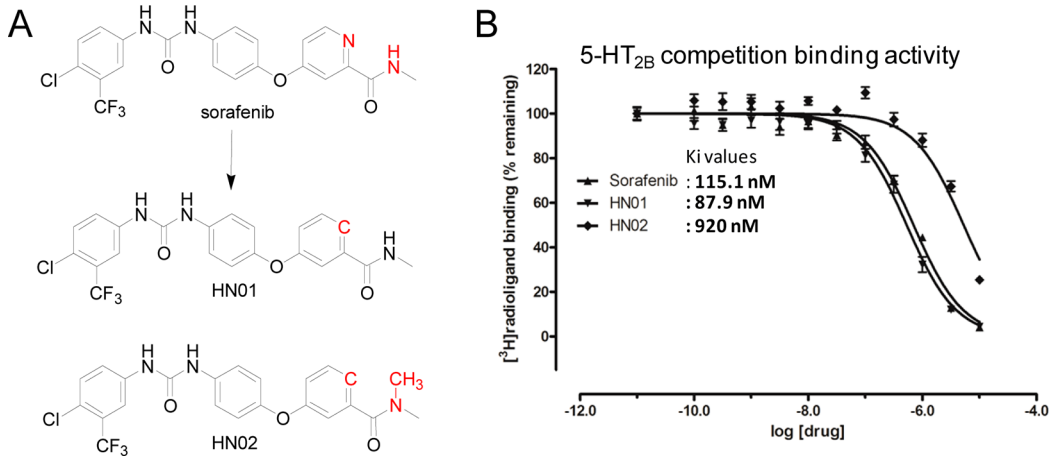

Figure 9. Chemical structures of designed sorafenib analogues (A) and their corresponding radioligand competition binding assay results (B). Note that the measured K_i value of sorafenib in this binding assay is 115.1 nM, different from our reported value of 56 nM. It is due to a new batch of 5-HT_{2B} pellets used in this new assay, where the K_d value of radioligand [^{3}H]-LSD is 0.97 nM, and 0.5 nM for the previously used batch. Thus, the measured sorafenib binding affinity values are consistent in both experiments.

binding modes, sorafenib has very different binding characteristics regarding its numerous polar interactions with binding site residues. Its hydrophobic trifluoromethylphenyl unit is buried in the hydrophobic site 1 and might contribute largely to ligand binding. Remarkably, it does not contain a positively charged nitrogen atom; instead, it forms strong hydrogen bonds between amide nitrogen atoms of its urea moiety to the carboxylate group of $D_{3.32}$. Other polar interactions include hydrogen bonds between its methyl amide oxygen atom to the hydroxyl group of $T_{2.64}$ and amide nitrogen atom of $Asn_{7.36}$, also its methyl amide nitrogen donates a hydrogen bond to the main chain carbonyl of $L_{7.35}$. It is interesting that the amide nitrogen atoms of the urea moiety form exactly the same interaction with the carboxylate group of the residue E500 in sorafenib–kinase crystal complex structures.[72] The binding details of sorafenib with BRAF kinase (PDB code: 1UWH) are illustrated in Figure 8B. It is not likely that the lack of a positively charged group largely reduces the binding affinity between sorafenib and 5-HT_{2A}, as its binding to 5-HT_{2B} is at low nanomolar range, where this selectivity may be caused by the other variable binding-site residues like the 5.46 position residue (a serine in 5-HT_{2A}, while an alanine in 5-HT_{2B} and 5-HT_{2C}) just as the ergoline compounds.[70] This is consistent with a recent report where Ladduwahetty and co-workers discovered novel 5-HT_{2A} receptor antagonists without containing any positively charged groups.[73] Nevertheless, it is likely that sorafenib can be used as a novel 5-HT_{2A} lead compound for further structural optimization with maintaining the biaryl urea structural moiety. As the ligand similarity-based SEA method has been successfully applied in identifying GPCR related off-targets, the receptor structure-based docking method may become a complementary approach for GPCR drug off-target discovery when the receptor structure is available or can be reliably modeled. Nevertheless, well designed experimental mutagenesis studies and the development of more accurate 5-HT_{2A}–sorafenib structure models are desirable for further investigation of the binding details at the atomic level.

As a proof-of-concept study, we designed series of sorafenib analogues to assess the predicted binding mode; two of them (Figure 9A) have been synthesized and evaluated against 5-HT_{2B} receptor (Figure 9B). The chemical synthesis route and analysis data are reported in Supporting Information. The replacement of aromatic nitrogen atom to carbon atom in compound HN01, leads to slight improvement of binding, which indicates that the aromatic nitro atom does not form direct polar interaction with receptor. The addition of methyl group on amide nitrogen atom in compound HN02 removes its potential hydrogen bond to the main chain carbonyl of $L_{7.35}$ and leads to 8-fold loss of binding. Both modifications strongly support the predicted binding mode of sorafenib. The complete

dx.doi.org/10.1021/jm300338m | J. Med. Chem. 2012, 55, 5749–5759

SAR exploration on sorafenib will be pursued and published at somewhere else.

New Clinical Implication of Sorafenib. Sorafenib is well-known to produce anticancer effects through targeting multiple kinases. Sorafenib was originally developed as a RAF-kinase inhibitor (52 nM) but subsequently has been shown to be a multikinase inhibitor that also inhibits PDGFRβ (37 nM), VEGFR2 (59 nM), VEGFR3 (16 nM), c-Kit (31 nM), and FLT1 (31 nM).[74] 5-HT_{2B} is highly expressed in the liver, kidneys, stomach, and gut.[12] Considering that the 5-HT_{2B} binding affinity of sorafenib is in the same therapeutic window as its kinase inhibition activities, one may hypothesize that the 5-HT_{2B} inhibition might directly contribute to the anticancer effect of sorafenib; in this regard, we have previously suggested that 5-HT_{2B} antagonists might be of special benefit for carcinoid tumors and sorafenib might represent a novel treatment for this disorder.[75] Nevertheless, recent studies have suggested that 5-HT receptors may be involved in the cell viability and cell cycle progression in certain cancers, especially for liver cancer and carcinoid-like tumors.[76−78] Sorafenib was approved to treat advanced renal cell carcinoma (RCC) and hepatocellular carcinoma (HCC), and intriguingly, 5-HT was suggested to promote cell survival and growth of HCC cells by activation of the 5-HT_{2B} receptor.[78] However, we cannot exclude the possibility that the 5-HTR activities of sorafenib might also cause side effects instead of bringing clinical benefits in certain circumstances. Although it is well beyond the scope of our current study, it is desirable to dissect the contributions of kinase inhibitions and 5-HTR antagonist activities in sorafenib-produced anticancer effect; as such information may facilitate clinical usage of sorafenib as well as designing new drugs with better anticancer efficacy and fewer side effects.

4. CONCLUSION

Drug profiling campaigns have revealed novel polypharmacology of existing drugs. It is critical to fully understand the target binding profile of a drug molecule, as its potential off-target binding properties may lead to better clinical efficacy in certain circumstances while causing side effects in other cases. GPCRs and kinases are two of the most important drug target families, and many of their ligands have been discovered to have promiscuous binding propensities within their own protein families. However, as far as we are aware, the ligand cross-reactivity between GPCR orthosteric ligand and kinase inhibitor has not been previously reported.

To predict novel polypharmacology, we computationally screened the FDA approved drug molecules against the induced-fit models of the 5-HT_{2A} receptor. We employed a comprehensive "induced-fit" protocol to simulate the receptor conformational changes upon binding with two representative 5-HT_{2A} antagonists, where different computational techniques were integrated systematically, including homology modeling, molecular docking, side chain prediction, and molecular dynamics in explicit membrane and solvent conditions. The multiple independent simulations with the presence of different ligand docking poses lead to the best quality structural models which satisfy the available experimental evidence and achieve the best docking performance by enriching the known ligands from decoy molecules in retrospective virtual screening. Such identified induced-fit models were used in docking screening of FDA drug molecules, with a total of six drug molecules chosen for experimental binding assay. Surprisingly, a well-known multikinase inhibitor, sorafenib has shown relatively strong binding affinity to 5-HT_{2A}, and subsequent 5-HTR profiling results indicate its promiscuous 5-HTRs inhibition activities. Whether or not the off-target inhibition of 5-HTRs by sorafenib has any clinical relevance has yet to be determined. However, it is desirable to dissect the contributions of kinase inhibitions and 5-HTR antagonist activities in sorafenib-produced anticancer effects. Ultimately, we can also envision a strategy to virtual screening GPCR ligands against therapeutically relevant kinases, and ask whether we could discover known GPCR ligands with unexpected kinase activities.

Interestingly, the structural characteristics of sorafenib are distinct to classic 5-HT_{2A} antagonists, especially considering the lack of the tertiary amine to form the salt-bridge interaction with the critical binding-site residue $D_{3.32}$. Instead, sorafenib may form strong hydrogen bonds between amide nitrogen atoms of its urea moiety to carboxylate group of $D_{3.32}$, and it may also form additional hydrogen bonds between its methyl amide with binding site residues. Nevertheless, the biaryl urea moiety may suggest new direction for developing novel 5-HTR ligands.

■ ASSOCIATED CONTENT

Ⓢ Supporting Information

The sequence alignment between 5-HT_{2A} and its template β-2 adrenoceptor, the structural descriptors used to evaluate the ketanserin complex system, the chemical structure and docking pose prediction assessment of ketanserin-like and cyproheptadine-like ligands, the ranks and annotated activities of top scored docking hits, the structures and experimental binding data of six FDA approved drugs, the detailed experimental assay protocols, and the chemical synthesis route for sorafenib analogues and their corresponding analysis data. This material is available free of charge via the Internet at http://pubs.acs.org.

■ AUTHOR INFORMATION

Corresponding Author

*Phone: 86-10-80720645. Fax: 86-10-80720813. E-mail: huangniu@nibs.ac.cn.

Notes

The authors declare no competing financial interest.

■ ACKNOWLEDGMENTS

We thank the reviewers for their constructive comments for improving the manuscript. Financial support from the Chinese Ministry of Science and Technology "973" grant 2011CB812402 (to N.H.) is gratefully acknowledged. B.L.R., R.W., and X-P.H. were supported by RO1MH82441 and the NIMH Psychoactive Drug Screening Program (PDSP). Computational support was provided by the Supercomputing Center of Chinese Academy of Sciences (SCCAS) and the Beijing Computing Center (BCC). We also thank Dr. Pearl Huang at BeiGene LTD for reading the manuscript and advice and Dr. Andrew Christofferson for proofreading.

■ ABBREVIATIONS USED

CNS, central nervous system; GPCRs, G protein-coupled receptors; 5-HTRs, 5-hydroxytryptamine receptors; β2-AR, β2-adrenoceptor; ECL2, extracellular loop 2; TM, transmembrane helix; PLOP, Protein Local Optimization Program; MD, molecular dynamics; PME, particle mesh Ewald; RMSDs, root-mean-square differences; SEA, similarity ensemble approach; PDSP, Psychoactive Drug Screening Program; SAR,

structure−activity relationship; EF, enrichment factor; LC-MS, liquid chromatography−mass spectrometry; NMR, nuclear magnetic resonance; RCC, advanced renal cell carcinoma; HCC, hepatocellular carcinoma

REFERENCES

(1) Roth, B. L.; Sheffler, D. J.; Kroeze, W. K. Magic shotguns versus magic bullets: selectively non-selective drugs for mood disorders and schizophrenia. *Nature Rev. Drug Discovery* **2004**, *3*, 353−359.

(2) Sams-Dodd, F. Target-based drug discovery: is something wrong? *Drug Discovery Today* **2005**, *10*, 139−147.

(3) Weber, A.; Casini, A.; Heine, A.; Kuhn, D.; Supuran, C. T.; Scozzafava, A.; Klebe, G. Unexpected nanomolar inhibition of carbonic anhydrase by COX-2-selective celecoxib: new pharmacological opportunities due to related binding site recognition. *J. Med. Chem.* **2004**, *47*, 550−557.

(4) Capdeville, R.; Buchdunger, E.; Zimmermann, J.; Matter, A. Glivec (STI571, imatinib), a rationally developed, targeted anticancer drug. *Nature Rev. Drug Discovery* **2002**, *1*, 493−502.

(5) Fabian, M. A.; Biggs, W. H., III; Treiber, D. K.; Atteridge, C. E.; Azimioara, M. D.; Benedetti, M. G.; Carter, T. A.; Ciceri, P.; Edeen, P. T.; Floyd, M.; Ford, J. M.; Galvin, M.; Gerlach, J. L.; Grotzfeld, R. M.; Herrgard, S.; Insko, D. E.; Insko, M. A.; Lai, A. G.; Lelias, J. M.; Mehta, S. A.; Milanov, Z. V.; Velasco, A. M.; Wodicka, L. M.; Patel, H. K.; Zarrinkar, P. P.; Lockhart, D. J. A small molecule−kinase interaction map for clinical kinase inhibitors. *Nature Biotechnol.* **2005**, *23*, 329−336.

(6) Xie, L.; Wang, J.; Bourne, P. E. In silico elucidation of the molecular mechanism defining the adverse effect of selective estrogen receptor modulators. *PLoS Comput. Biol.* **2007**, *3*, e217.

(7) Keiser, M. J.; Roth, B. L.; Armbruster, B. N.; Ernsberger, P.; Irwin, J. J.; Shoichet, B. K. Relating protein pharmacology by ligand chemistry. *Nature Biotechnol.* **2007**, *25*, 197−206.

(8) Liu, X.; Ouyang, S.; Yu, B.; Liu, Y.; Huang, K.; Gong, J.; Zheng, S.; Li, Z.; Li, H.; Jiang, H. PharmMapper server: a web server for potential drug target identification using pharmacophore mapping approach. *Nucleic. Acids. Res.* **2009**, No. Suppl, 38−614.

(9) Yang, L.; Chen, J.; Shi, L.; Hudock, M. P.; Wang, K.; He, L. Identifying unexpected therapeutic targets via chemical−protein interactome. *PLoS One* **2010**, *5*, e9568.

(10) Yadav, P. N.; Kroeze, W. K.; Farrell, M. S.; Roth, B. L. Antagonist functional selectivity: 5-HT2A serotonin receptor antagonists differentially regulate 5-HT2A receptor protein level in vivo. *J. Pharmacol. Exp. Ther.* **2011**, *339*, 99−105.

(11) Lowrie, J. F.; Delisle, R. K.; Hobbs, D. W.; Diller, D. J. The different strategies for designing GPCR and kinase targeted libraries. *Comb. Chem. High Throughput Screening* **2004**, *7*, 495−510.

(12) Nichols, D. E.; Nichols, C. D. Serotonin receptors. *Chem. Rev.* **2008**, *108*, 1614−1641.

(13) Sharpley, A. L.; Elliott, J. M.; Attenburrow, M. J.; Cowen, P. J. Slow wave sleep in humans: role of 5-HT2A and 5-HT2C receptors. *Neuropharmacology* **1994**, *33*, 467−471.

(14) Salmi, P.; Ahlenius, S. Evidence for functional interactions between 5-HT1A and 5-HT2A receptors in rat thermoregulatory mechanisms. *Pharmacol. Toxicol.* **1998**, *82*, 122−127.

(15) Nacmias, B.; Ricca, V.; Tedde, A.; Mezzani, B.; Rotella, C. M.; Sorbi, S. 5-HT2A receptor gene polymorphisms in anorexia nervosa and bulimia nervosa. *Neurosci. Lett.* **1999**, *277*, 134−136.

(16) Nagatomo, T.; Rashid, M.; Abul Muntasir, H.; Komiyama, T. Functions of 5-HT2A receptor and its antagonists in the cardiovascular system. *Pharmacol. Ther.* **2004**, *104*, 59−81.

(17) Roth, B. L.; Willins, D. L.; Kristiansen, K.; Kroeze, W. K. 5-Hydroxytryptamine2-family receptors (5-hydroxytryptamine2A, 5-hydroxytryptamine2B, 5-hydroxytryptamine2C): where structure meets function. *Pharmacol. Ther.* **1998**, *79*, 231−257.

(18) Rowley, M.; Bristow, L. J.; Hutson, P. H. Current and novel approaches to the drug treatment of schizophrenia. *J. Med. Chem.* **2001**, *44*, 477−501.

(19) Congreve, M.; Langmead, C. J.; Mason, J. S.; Marshall, F. H. Progress in structure based drug design for G protein-coupled receptors. *J. Med. Chem.* **2011**, *54*, 4283−4311.

(20) Palczewski, K.; Kumasaka, T.; Hori, T.; Behnke, C. A.; Motoshima, H.; Fox, B. A.; Le Trong, I.; Teller, D. C.; Okada, T.; Stenkamp, R. E.; Yamamoto, M.; Miyano, M. Crystal structure of rhodopsin: A G protein-coupled receptor. *Science* **2000**, *289*, 739−745.

(21) Congreve, M.; Marshall, F. The impact of GPCR structures on pharmacology and structure-based drug design. *Br. J. Pharmacol.* **2009**, *159*, 986−996.

(22) Li, Y. Y.; Hou, T. J.; Goddard, W. A., III. Computational modeling of structure−function of g protein-coupled receptors with applications for drug design. *Curr. Med. Chem.* **2010**, *17*, 1167−1180.

(23) Costanzi, S. On the applicability of GPCR homology models to computer-aided drug discovery: a comparison between in silico and crystal structures of the beta2-adrenergic receptor. *J. Med. Chem.* **2008**, *51*, 2907−2914.

(24) Senderowitz, H.; Marantz, Y. G Protein-Coupled Receptors: target-based in silico screening. *Curr. Pharm. Des.* **2009**, *15*, 4049−4068.

(25) Mobarec, J. C.; Sanchez, R.; Filizola, M. Modern homology modeling of G-protein coupled receptors: which structural template to use? *J. Med. Chem.* **2009**, *52*, 5207−5216.

(26) Yarnitzky, T.; Levit, A.; Niv, M. Y. Homology modeling of G-protein-coupled receptors with X-ray structures on the rise. *Curr. Opin. Drug Discovery Dev.* **2010**, *13*, 317−325.

(27) Phatak, S. S.; Gatica, E. A.; Cavasotto, C. N. Ligand-steered modeling and docking: a benchmarking study in class A G-protein-coupled receptors. *J. Chem. Inf. Model.* **2010**, *50*, 2119−2128.

(28) McRobb, F. M.; Capuano, B.; Crosby, I. T.; Chalmers, D. K.; Yuriev, E. Homology modeling and docking evaluation of aminergic G protein-coupled receptors. *J. Chem. Inf. Model.* **2010**, *50*, 626−637.

(29) Carlsson, J.; Coleman, R. G.; Setola, V.; Irwin, J. J.; Fan, H.; Schlessinger, A.; Sali, A.; Roth, B. L.; Shoichet, B. K. Ligand discovery from a dopamine D3 receptor homology model and crystal structure. *Nature Chem. Biol.* **2011**, *7*, 769−778.

(30) Hanson, M. A.; Cherezov, V.; Griffith, M. T.; Roth, C. B.; Jaakola, V. P.; Chien, E. Y.; Velasquez, J.; Kuhn, P.; Stevens, R. C. A specific cholesterol binding site is established by the 2.8 A structure of the human beta2-adrenergic receptor. *Structure* **2008**, *16*, 897−905.

(31) Sali, A.; Blundell, T. L. Comparative protein modelling by satisfaction of spatial restraints. *J. Mol. Biol.* **1993**, *234*, 779−815.

(32) Horn, F.; Weare, J.; Beukers, M. W.; Horsch, S.; Bairoch, A.; Chen, W.; Edvardsen, O.; Campagne, F.; Vriend, G. GPCRDB: an information system for G protein-coupled receptors. *Nucleic Acids Res.* **1998**, *26*, 275−279.

(33) Marchler-Bauer, A.; Lu, S.; Anderson, J. B.; Chitsaz, F.; Derbyshire, M. K.; DeWeese-Scott, C.; Fong, J. H.; Geer, L. Y.; Geer, R. C.; Gonzales, N. R.; Gwadz, M.; Hurwitz, D. I.; Jackson, J. D.; Ke, Z.; Lanczycki, C. J.; Lu, F.; Marchler, G. H.; Mullokandov, M.; Omelchenko, M. V.; Robertson, C. L.; Song, J. S.; Thanki, N.; Yamashita, R. A.; Zhang, D.; Zhang, N.; Zheng, C.; Bryant, S. H. CDD: A Conserved Domain Database for the Functional Annotation of Proteins. *Nucleic Acids Res.* **2010**, *39*, D225−229.

(34) Varady, J.; Wu, X.; Fang, X.; Min, J.; Hu, Z.; Levant, B.; Wang, S. Molecular modeling of the three-dimensional structure of dopamine 3 (D3) subtype receptor: discovery of novel and potent D3 ligands through a hybrid pharmacophore- and structure-based database searching approach. *J. Med. Chem.* **2003**, *46*, 4377−4392.

(35) Evers, A.; Klabunde, T. Structure-based drug discovery using GPCR homology modeling: successful virtual screening for antagonists of the alpha1A adrenergic receptor. *J. Med. Chem.* **2005**, *48*, 1088−1097.

(36) Sherman, W.; Day, T.; Jacobson, M. P.; Friesner, R. A.; Farid, R. Novel procedure for modeling ligand/receptor induced fit effects. *J. Med. Chem.* **2006**, *49*, 534−553.

(37) Evers, A.; Klebe, G. Ligand-supported homology modeling of G protein-coupled receptor sites: models sufficient for successful virtual screening. *Angew. Chem., Int. Ed. Engl.* **2004**, *43*, 248−251.

(38) Lorber, D. M.; Shoichet, B. K. Flexible ligand docking using conformational ensembles. *Protein Sci.* **1998**, *7*, 938−950.
(39) Wei, B. Q.; Baase, W. A.; Weaver, L. H.; Matthews, B. W.; Shoichet, B. K. A model binding site for testing scoring functions in molecular docking. *J. Mol. Biol.* **2002**, *322*, 339−355.
(40) Gloriam, D. E.; Foord, S. M.; Blaney, F. E.; Garland, S. L. Definition of the G protein-coupled receptor transmembrane bundle binding pocket and calculation of receptor similarities for drug design. *J. Med. Chem.* **2009**, *52*, 4429−4442.
(41) Huang, N.; Shoichet, B. K.; Irwin, J. J. Benchmarking Sets for Molecular Docking. *J. Med. Chem.* **2006**, *49*, 6789−6801.
(42) Irwin, J. J.; Shoichet, B. K.; Mysinger, M. M.; Huang, N.; Colizzi, F.; Wassam, P.; Cao, Y. Automated docking screens: a feasibility study. *J. Med. Chem.* **2009**, *52*, 5712−5720.
(43) Lorber, D. M.; Shoichet, B. K. Hierarchical docking of databases of multiple ligand conformations. *Curr. Top. Med. Chem.* **2005**, *5*, 739−749.
(44) Ester, M.; Kriegel, H. P.; Sander, J.; Xu, X. W. A density-based algorithm for discovering clusters in large spatial databases with noise. In *Proceedings of the Second International Conference on Knowledge Discovery and Data Mining*; Simoudis, E., Han, J., Fayyad, U. M., Eds.; AAAI Press: Palo Alto, CA, 1995; pp 226−231.
(45) Bernacki, K.; Kalyanaraman, C.; Jacobson, M. P. Virtual ligand screening against *Escherichia coli* dihydrofolate reductase: improving docking enrichment using physics-based methods. *J. Biomol. Screening* **2005**, *10*, 675−681.
(46) Kalyanaraman, C.; Bernacki, K.; Jacobson, M. P. Virtual screening against highly charged active sites: identifying substrates of alpha−beta barrel enzymes. *Biochemistry* **2005**, *44*, 2059−2071.
(47) Huang, N.; Kalyanaraman, C.; Bernacki, K.; Jacobson, M. P. Molecular mechanics methods for predicting protein−ligand binding. *Phys. Chem. Chem. Phys.* **2006**, *8*, 5166−5177.
(48) Huang, N.; Kalyanaraman, C.; Irwin, J. J.; Jacobson, M. P. Physics-based scoring of protein−ligand complexes: enrichment of known inhibitors in large-scale virtual screening. *J. Chem. Inf. Model.* **2006**, *46*, 243−253.
(49) Huang, N.; Jacobson, M. P. Binding-site assessment by virtual fragment screening. *PLoS One* **2010**, *5*, e10109.
(50) Rapp, C. S.; Schonbrun, C.; Jacobson, M. P.; Kalyanaraman, C.; Huang, N. Automated site preparation in physics-based rescoring of receptor ligand complexes. *Proteins* **2009**, *77*, 52−61.
(51) Jacobson, M. P.; Kaminski, G. A.; Friesner, R. A.; Rapp, C. A. Force field validation using protein side chain prediction. *J. Phys. Chem. B* **2002**, *106*, 11673−11680.
(52) Jacobson, M. P.; Pincus, D. L.; Rapp, C. S.; Day, T. J.; Honig, B.; Shaw, D. E.; Friesner, R. A. A hierarchical approach to all-atom protein loop prediction. *Proteins* **2004**, *55*, 351−367.
(53) Li, X.; Jacobson, M. P.; Friesner, R. A. High-resolution prediction of protein helix positions and orientations. *Proteins* **2004**, *55*, 368−382.
(54) Kevin, J. B.; Edmond, C.; Huafeng, X.; Ron, O. D.; Michael, P. E.; Brent, A. G.; John, L. K.; István, K.; Mark, A. M.; Federico, D. S.; John, K. S.; Yibing, S.; David, E. S. Scalable algorithms for molecular dynamics simulations on commodity clusters. Proceedings of the ACM/IEEE Conference on Supercomputing (SC06), Tampa, FL, November 11−17, 2006.
(55) Banks, J. L.; Beard, H. S.; Cao, Y.; Cho, A. E.; Damm, W.; Farid, R.; Felts, A. K.; Halgren, T. A.; Mainz, D. T.; Maple, J. R.; Murphy, R.; Philipp, D. M.; Repasky, M. P.; Zhang, L. Y.; Berne, B. J.; Friesner, R. A.; Gallicchio, E.; Levy, R. M. Integrated Modeling Program, Applied Chemical Theory (IMPACT). *J. Comput. Chem.* **2005**, *26*, 1752−1780.
(56) Kräutler, V.; van Gunsteren, W. F.; Hünenberger, P. H. A fast SHAKE algorithm to solve distance constraint equations for small molecules in molecular dynamics simulations. *J. Comput. Chem.* **2001**, *22*, 501−508.
(57) Darden, T.; York, D.; Pedersen, L. Particle mesh Ewald: An *N* log(*N*) method for Ewald sums in large systems. *J. Chem. Phys.* **1993**, *98*, 10089−10092.
(58) Pettersen, E. F.; Goddard, T. D.; Huang, C. C.; Couch, G. S.; Greenblatt, D. M.; Meng, E. C.; Ferrin, T. E. UCSF Chimera—a visualization system for exploratory research and analysis. *J. Comput. Chem.* **2004**, *25*, 1605−1612.
(59) Humphrey, W.; Dalke, A.; Schulten, K. VMD: visual molecular dynamics. *J. Mol. Graphics* **1996**, *14*, 33−38.
(60) Irwin, J. J.; Shoichet, B. K. ZINC—a free database of commercially available compounds for virtual screening. *J. Chem. Inf. Model.* **2005**, *45*, 177−182.
(61) Wishart, D. S.; Knox, C.; Guo, A. C.; Shrivastava, S.; Hassanali, M.; Stothard, P.; Chang, Z.; Woolsey, J. DrugBank: a comprehensive resource for in silico drug discovery and exploration. *Nucleic Acids Res.* **2006**, *34*, D668−672.
(62) Overington, J. ChEMBL. An interview with John Overington, team leader, chemogenomics at the European Bioinformatics Institute Outstation of the European Molecular Biology Laboratory (EMBL-EBI). Interview by Wendy A. Warr. *J. Comput.-Aided Mol. Des.* **2009**, *23*, 195−198.
(63) Keiser, M. J.; Setola, V.; Irwin, J. J.; Laggner, C.; Abbas, A. I.; Hufeisen, S. J.; Jensen, N. H.; Kuijer, M. B.; Matos, R. C.; Tran, T. B.; Whaley, R.; Glennon, R. A.; Hert, J.; Thomas, K. L.; Edwards, D. D.; Shoichet, B. K.; Roth, B. L. Predicting new molecular targets for known drugs. *Nature* **2009**, *462*, 175−181.
(64) Surgand, J. S.; Rodrigo, J.; Kellenberger, E.; Rognan, D. A chemogenomic analysis of the transmembrane binding cavity of human G protein-coupled receptors. *Proteins* **2006**, *62*, 509−538.
(65) Runyon, S. P.; Mosier, P. D.; Roth, B. L.; Glennon, R. A.; Westkaemper, R. B. Potential modes of interaction of 9-aminomethyl-9,10-dihydroanthracene (AMDA) derivatives with the 5-HT2A receptor: a ligand structure−affinity relationship, receptor mutagenesis and receptor modeling investigation. *J. Med. Chem.* **2008**, *51*, 6808−6828.
(66) Shi, L.; Javitch, J. A. The binding site of aminergic G protein-coupled receptors: the transmembrane segments and second extracellular loop. *Annu. Rev. Pharmacol. Toxicol.* **2002**, *42*, 437−467.
(67) Roth, B. L.; Shoham, M.; Choudhary, M. S.; Khan, N. Identification of conserved aromatic residues essential for agonist binding and second messenger production at 5-hydroxytryptamine2A receptors. *Mol. Pharmacol.* **1997**, *52*, 259−266.
(68) Choudhary, M. S.; Craigo, S.; Roth, B. L. A single point mutation (Phe340→Leu340) of a conserved phenylalanine abolishes 4-[125I]iodo-(2,5-dimethoxy)phenylisopropylamine and [3H]-mesulergine but not [3H]ketanserin binding to 5-hydroxytryptamine2 receptors. *Mol. Pharmacol.* **1993**, *43*, 755−761.
(69) Almaula, N.; Ebersole, B. J.; Zhang, D.; Weinstein, H.; Sealfon, S. C. Mapping the binding site pocket of the serotonin 5-hydroxytryptamine2A receptor. Ser3.36(159) provides a second interaction site for the protonated amine of serotonin but not of lysergic acid diethylamide or bufotenin. *J. Biol. Chem.* **1996**, *271*, 14672−14675.
(70) Almaula, N.; Ebersole, B. J.; Ballesteros, J. A.; Weinstein, H.; Sealfon, S. C. Contribution of a helix 5 locus to selectivity of hallucinogenic and nonhallucinogenic ligands for the human 5-hydroxytryptamine2A and 5-hydroxytryptamine2C receptors: direct and indirect effects on ligand affinity mediated by the same locus. *Mol. Pharmacol.* **1996**, *50*, 34−42.
(71) Westkaemper, R. B.; Glennon, R. A. Application of ligand SAR, receptor modeling and receptor mutagenesis to the discovery and development of a new class of 5-HT(2A) ligands. *Curr. Top. Med. Chem.* **2002**, *2*, 575−598.
(72) Wan, P. T.; Garnett, M. J.; Roe, S. M.; Lee, S.; Niculescu-Duvaz, D.; Good, V. M.; Jones, C. M.; Marshall, C. J.; Springer, C. J.; Barford, D.; Marais, R. Mechanism of activation of the RAF-ERK signaling pathway by oncogenic mutations of B-RAF. *Cell* **2004**, *116*, 855−867.
(73) Ladduwahetty, T.; Gilligan, M.; Humphries, A.; Merchant, K. J.; Fish, R.; McAlister, G.; Ivarsson, M.; Dominguez, M.; O'Connor, D.; MacLeod, A. M. Non-basic ligands for aminergic GPCRs: the discovery and development diaryl sulfones as selective, orally

bioavailable 5-HT2A receptor antagonists for the treatment of sleep disorders. *Bioorg. Med. Chem. Lett.* **2010**, *20*, 3708−3712.
(74) Karaman, M. W.; Herrgard, S.; Treiber, D. K.; Gallant, P.; Atteridge, C. E.; Campbell, B. T.; Chan, K. W.; Ciceri, P.; Davis, M. I.; Edeen, P. T.; Faraoni, R.; Floyd, M.; Hunt, J. P.; Lockhart, D. J.; Milanov, Z. V.; Morrison, M. J.; Pallares, G.; Patel, H. K.; Pritchard, S.; Wodicka, L. M.; Zarrinkar, P. P. A quantitative analysis of kinase inhibitor selectivity. *Nature Biotechnol.* **2008**, *26*, 127−132.
(75) Roth, B. L. Drugs and valvular heart disease. *N. Engl. J. Med.* **2007**, *356*, 6−9.
(76) Oufkir, T.; Arseneault, M.; Sanderson, J. T.; Vaillancourt, C. The 5-HT2A serotonin receptor enhances cell viability, affects cell cycle progression and activates MEK-ERK1/2 and JAK2-STAT3 signalling pathways in human choriocarcinoma cell lines. *Placenta* **2010**, *31*, 439−447.
(77) Asada, M.; Ebihara, S.; Yamanda, S.; Niu, K.; Okazaki, T.; Sora, I.; Arai, H. Depletion of serotonin and selective inhibition of 2B receptor suppressed tumor angiogenesis by inhibiting endothelial nitric oxide synthase and extracellular signal-regulated kinase 1/2 phosphorylation. *Neoplasia* **2009**, *11*, 408−417.
(78) Soll, C.; Jang, J. H.; Riener, M. O.; Moritz, W.; Wild, P. J.; Graf, R.; Clavien, P. A. Serotonin promotes tumor growth in human hepatocellular cancer. *Hepatology* **2010**, *51*, 1244−1254.